# The libron–phonon coupling and the IR absorption spectra of diatomic molecules in a simple liquid

I. L. Garzón
*Instituto de Física, Universidad Nacional Autónoma de México, A.P. 20-364, 01000 México, D.F., México*

Estela Blaisten-Barojas[a]
*Department of Chemistry, Stanford University, Stanford, California 94305*

S. Fujita
*Department of Physics and Astronomy, State University of New York at Buffalo, Amherst, New York 14260*

The IR absorption coefficient for diatomic impurities dissolved in liquid solutions is calculated from a $3D$ model Hamiltonian. The liquid atoms surrounding the impurity form a cage that hinders strongly the molecular rotation reducing it to a librational motion. The coupling between the collective motion of the liquid and the impurity-librational motion generates the libron–phonon interaction. The shifts and broadenings of the IR spectral lines are calculated on the basis of linear response theory with a proper connected diagram analysis. Recent experimental IR measurements for CO and ClF in liquid argon are analyzed in terms of the present theory and the strength of the libron–phonon coupling for such systems is reported.

## I. INTRODUCTION

There has been considerable interest in the study of the librational motion of molecular impurities in dense media due primarily to the desire to account for the appropriate mechanisms of interaction. Much of the experimental work has been the use of near IR spectroscopy of diatomics in dense gases,[1] liquids,[2,3] or trapped in solid matrices.[4] Experiments on solutions were performed by Buontempo et al.[2] and Chandler and Ewing[3] for CO in liquid Ar at 97 and 85 K and by Naulin et al.[5] for ClF in liquid Ar, $N_2$, and $O_2$ at various temperatures, among others. In liquid solutions, all measured IR absorption spectra show a broad central band and two weak shoulders towards the high and low frequency regions.

In this paper, we concentrate on the IR absorption theory of polar diatomic solutes with large moment of inertia in nonpolar liquid solvents. Recently Berens and Wilson[6] proposed a fit for the near IR spectra of gaseous[1] and liquid[2] solutes in Ar based on a molecular dynamics calculation with *ad hoc* quantum corrections. Another model used recently for molecules trapped in solid matrices was the pseudorotating cage of Manz.[7] The existence of a cavity gives the static effect of the matrix neighboring atoms surrounding the impurity.

Dynamical approaches of diatomics in liquid solutions started with Robert and Galatry.[8] They used a cage model to mimic the liquid structure perturbing the molecular orientation within a quantum formulation. The atoms in the liquid surrounding the impurity are viewed as a thermal bath represented by a fluctuating potential.

This approach allows them to obtain the IR spectrum of HCl in liquid $CCl_4$ after fitting various parameters. More recently, Mauricio et al.[9] again used the idea of molecules in cages. This is a 2D dynamical model in which the cage interacts with a viscous isothermal bath through an indirect coupling between the librational motion of the molecule and phonons. These approaches do not give a microscopic description of the different interactions taking place in the system, but rather supply phenomenological descriptions. Other approaches better suited for solvents at room temperature and/or molecules with small moment of inertia, couple the molecular rotation to the environment via a stochastic potential,[10] or use rotational diffusion arguments.[11]

The model described in Sec. II pictures a diatomic molecule placed in a moving cage created by the surrounding atoms in the liquid. The cage effect is such that the rotation of the molecules is strongly perturbed resulting in a libration. This angular motion is coupled to the collective modes of the liquid giving rise to the libron–phonon coupling, as we have discussed previously in a 1D treatment.[12] In Sec. III the absorption coefficient for liquid solutions is obtained in the linear response regime,[13] whereas the 3D results for solid matrices are given elsewhere.[14] The Green's function of the dipole moment is calculated via the proper connected diagram analysis.[15] Finally, in Sec. IV we give a comparison of the resulting expressions with two experiments and conclude with a brief discussion.

## II. MODEL

Let us consider a solution of diatomic polar molecules ($D$) in simple liquids at low temperatures. We assume that the liquid surrounding $D$ generates a cage that

---

[a] Permanent address: Instituto de Física, Universidad Nacional Autónoma de México, A.P. 20-364, 01000 México, D.F., México.

strongly hinders $D$'s rotation. Inside the cage, $D$ is in a minimum energy configuration when the internuclear radius $r$ is along the $z$ direction as shown in Fig. 1. We further assume that the interaction molecule cage is strong enough to reduce $D$'s rotation to a libration. This assumption should be good when the molecular moment of inertia is large. At the cage center is $D$'s center of mass anchored in such a way that an instantaneous position of $D$ is given by $x$, $y$, $z$ (Fig. 1). We describe the above model in cylindrical coordinates fixed in the molecule, with the $z$ axes along $r$ when the molecule is at rest. Since for small angular displacements between $r$ and $z$, the moment of inertia along $z$ is very small, $D$'s kinetic energy can be written as

$$T_M = \frac{1}{2m_{AB}}(p_x^2 + p_y^2 + p_r^2),\qquad(1)$$

where $p_x = m_{AB}\dot{x}$, $p_y = m_{AB}\dot{y}$, $p_r = m_{AB}\dot{r}$ and $m_{AB} = m_A m_B/(m_A + m_B)$. In a classical liquid, the collective variables can be seen as normal modes for longitudinal sound propagation in a nonviscous fluid.[16] The actual time dependence of these variables is given by hydrodynamic laws, then they have long lifetimes. We can visualize these collective variables as oscillations of a chain of $N - 1$ atoms along the $x'$ direction (Fig. 1). The cage center occupies the $i$th position in this chain and is allowed to translate as any other atom in it. The cage center is thus following the collective behavior of the liquid. The total kinetic energy is

$$T = \sum_{\substack{s'=1\\s'\neq i}}^{N} \frac{p_{s'}^2}{2m} + \frac{p_i^2}{2(m_A + m_B)} + T_M.\qquad(2)$$

The interaction between $D$ and the liquid is accounted by (1) the formation of the cage that hinders $D$'s rotation



FIG. 1. Geometry of the molecule in its environment. $S$ is the coordinate system fixed in the molecule. $S'$ is the coordinate system chosen as to have the $x'$ axes along the $\mathbf{k}$ phonon vector direction. The $S'$ origin is arbitrarily displaced from the $S$ origin.

yielding a libration, and (2) the coupling of this libration to the collective coordinates. The potential energy is consequently expressed in the fixed system of coordinates as

$$V = V_1(\{\mathbf{d}_{s,s-1}\}) + V_2(r) + V_3(x, y)$$
$$+ V_4(\mathbf{d}_{i,i-1}, \mathbf{d}_{i+1,i}, x, y, r),\qquad(3)$$

where $V_1$ gives the liquid potential, $V_2$ stands for the intramolecular energy responsible for the molecular vibration of frequency $\omega_r$, $V_3$ represents the effect of the liquid in creating the cage and $V_4$ is the coupling between the librational motion and the liquid (libron–phonon interaction). This last function depends parametrically on the molecular interatomic distance $r$. The set of vectors $\{\mathbf{d}_{s,s-1}\}$ are the nearest-neighbor distances $x'_{s,s-1} \equiv x'_s - x'_{s-1}$ between two atoms projected onto the coordinate system fixed in the molecule (see Fig. 1). Among these distances are included those between the molecular center of mass and its two atomic neighbors.

Let us assume that (1) the longitudinal phonons are not perturbed by $D$, much in the same way as discussed previously;[12,17] (2) $V_3$ represents two harmonic potentials of the angular displacements (libration) with frequencies $\omega_x$ and $\omega_y$. These angular oscillators are not coupled to the molecular internal vibration of frequency $\omega_r$; (3) anharmonic terms in $x$ and $y$ will not be considered since we are concerned only with transitions deep into $V_3$ well; and (4) $V_4$ is Taylor-expanded up to second order in the angular and translational displacements,

$$V_4 = \sum_\eta k_\eta(\mathbf{d}_{i+1,i} - \mathbf{d}_{i,i-1})\cdot\Delta\eta,\qquad(4)$$

where $\eta = x, y$ and $\Delta\eta$ is a vector with components $\Delta x$, $\Delta y$ standing for the librational displacements and $k_\eta = (\partial^2 V_4/\partial x'_{i+1,i}\partial\eta)$. The $\theta_e$ and $\varphi_e$ dependence of Eq. (4) is eliminated only at the end of the calculation. In the past, we have shown[17] that the coupling between the molecular internal vibration and phonons is very small, so in Eq. (4) terms proportional to $\Delta z \sim \Delta r$ were neglected.

Summing up, the system looks like an unperturbed set of three harmonic oscillators with frequencies $\omega_x$, $\omega_y$, and $\omega_r$ plus a phonon field coupled via $V_4$ to give $H = H_0 + H_{int}$. In second quantization the unperturbed Hamiltonian can be written as

$$H_0 = \sum_\mathbf{k} \hbar\omega_\mathbf{k}\left(b_\mathbf{k}^+ b_\mathbf{k} + \frac{1}{2}\right) + \sum_{\eta=x,y,z} \hbar\omega_\eta\left(a_\eta^+ a_\eta + \frac{1}{2}\right)\qquad(5)$$

and the libron–phonon interaction term as

$$H_{int} = \sum_{\eta=x,y} \lambda_\eta \sum_\mathbf{k} F_\eta(\mathbf{k})(b_\mathbf{k}^+ + b_\mathbf{k})(a_\eta^+ + a_\eta),\qquad(6)$$

where

$$\lambda_\eta = k_\eta\left(\frac{\hbar}{2m_{AB}\omega_\eta}\right)^{1/2}\left(\frac{\hbar}{2m\omega_D}\right)^{1/2}$$

with $\omega_D$ the Debye cut-off frequency and

$$F_\eta(\mathbf{k}) = \frac{2}{\sqrt{N}}(\cos ka - 1)\left(\frac{\omega_D}{\omega_\mathbf{k}}\right)^{1/2} f_\eta,\qquad(7)$$

with $f_x = \sin\theta_l \cos\varphi_l$, $f_y = \sin\theta_l \sin\varphi_l$, and $a$ is an effective lattice constant. In addition, the following transformations[12] were used

$$\Delta x'_s = \sum_k \frac{e^{-i\mathbf{k}\cdot\mathbf{x}'_s}}{\sqrt{N}} \left(\frac{\hbar}{2m\omega_k}\right)^{1/2} (b_k^+ + b_k)$$

and

$$\Delta\eta = \left(\frac{\hbar}{2m_{AB}\omega_\eta}\right)^{1/2} (a_\eta^+ + a_\eta). \qquad (8)$$

The operators $a_\eta^+$, $a_\eta$, $b_k^+$, $b_k$ satisfy the usual boson commutation rules.

In the coordinate system fixed in the molecule the dipole moment components are

$$M_\eta = \mu(r)\frac{\Delta\eta}{r_e}, \quad \eta = x, y, z, \qquad (9)$$

with $\mu(r) = \mu_0 + \mu_1\Delta r$ and $r_e$ being the equilibrium intermolecular distance. As we have assumed that the $\Delta z$ displacements are mainly $\Delta r$, the $z$ component of the dipole moment is just $\mu(r)$. By rewriting Eq. (9) with the help of Eq. (8) the dipole moment operator is given by

$$M_\eta = m_\eta^+ a_\eta^+ + m_\eta^- a_\eta + m_\eta^{++} a_\eta^+ a_r^+$$
$$+ m_\eta^{+-} a_\eta^+ a_r + m_\eta^{-+} a_\eta a_r^+ + m_\eta^{--} a_\eta a_r, \qquad (10)$$

where $\eta = x, y, z$ and the constants $m$'s are defined in the Appendix. An expression similar to Eq. (10) is obtained for the current density operator $\hat{J} = \dot{M}$ when the $m$'s are replaced by the $j$'s defined in the Appendix as well.

## III. ABSORPTION COEFFICIENT

When an external and oscillating electric field of frequency $\omega$ is applied to the system described in Sec. II, the absorption coefficient is given by[12,18]

$$\alpha(\omega) = -\frac{E_0^2}{3}\frac{\omega}{v} \sum_{\eta=x,y,z} G''_\omega(M_\eta, M_\eta), \qquad (11)$$

where $E_0$ is the amplitude of the incident radiation, $v$ is the volume of the system and $G''_\omega(M_\eta, M_\eta)$ is the imaginary part of the Fourier transform of the dipole moment Green's function:

$$G(M_\eta(t), M_\eta) = -i\hbar^{-1}\theta(t)\langle[M_\eta(t), M_\eta]\rangle. \qquad (12)$$

Here $M_\eta(t)$ is the dipole moment $\eta$th component in the Heisenberg representation, $\theta(t)$ is the Heaviside function, and $\langle\cdots\rangle$ means the canonical ensemble average.

According to Kubo's formula[13,15] we can write $G_\omega(M_\eta, M_\eta)$, the Fourier transform of Eq. (12) as

$$G_\omega(M_\eta, M'_\eta) = -i\lim_{\epsilon\to 0}\frac{\partial}{\partial u'_\eta}\mathrm{Tr}\left\{\zeta'\frac{1}{\mathscr{H}-z}M_\eta\right\}\Big|_{u=0}, \qquad (13)$$

where

$$\rho' = Z^{-1}e^{-\beta(H-\mathbf{J}\cdot\mathbf{u})} \qquad (14)$$

and where $z = \omega - i\epsilon$, $\mathbf{J}$ is the current density, $\mathbf{u}$ is a constant vector, $\mathscr{H}$ is the Liouville operator $\mathscr{H}\theta = [H, \theta]$ denoted by script and $Z = \mathrm{Tr}\exp[-\beta(H - \mathbf{J}\cdot\mathbf{u})]$. Within

the weak coupling approximation we can evaluate $G_\omega(M_\eta, M_\eta)$ in terms of second-order proper connected diagrams.[15,19] This approximation is good if the density of impurities is low and the libron–phonon interaction is small. Using this approximation $\zeta'$ becomes

$$\rho'_0 = \frac{e^{-\beta(H_0 - \mathbf{J}\cdot\mathbf{u})}}{\mathrm{Tr}\{e^{-\beta(H_0-\mathbf{J}\cdot\mathbf{u})}\}} \qquad (15)$$

and $(\mathscr{H} - z)^{-1}$ transforms into $(\mathscr{H}_0 - z - b)^{-1}$ when one introduces the identity

$$b \equiv \mathscr{H}_{\mathrm{int}}(\mathscr{H}_0 - z - b)^{-1}\mathscr{H}_{\mathrm{int}}. \qquad (16)$$

Then, Eq. (13) can be written as

$$G_\omega(M_\eta, M_\eta)$$
$$= -i\lim_{\epsilon\to 0}\sum_{\nu_1,\nu_2}\left\langle\nu_2\left|\left(\frac{\partial\zeta'_0}{\partial u_\eta}\right)_{u_\eta=0}\right|\nu_1\right\rangle$$
$$\times\langle\nu_1|(\mathscr{H}_0 - z - b)^{-1}M_\eta|\nu_2\rangle. \qquad (17)$$

The summation runs over the $\nu_1$, $\nu_2$ states of the three molecular oscillators with eigenvalues

$$\epsilon_{\nu_j} = \sum_{\eta=x,y,r}\hbar\omega_\eta(n_{j\eta} + \tfrac{1}{2}), \qquad (18)$$

$j = 1, 2$ and $n_{j\eta} = 0, 1, 2, \ldots$.

Upon substitution of Eq. (10) into Eq. (11), and considering only resonant terms, the absorption coefficient is reduced to three components:

$$\alpha(\omega) = \alpha^-(\omega) + \alpha^{+-}(\omega) + \alpha^{--}(\omega), \qquad (19)$$

each one corresponding to a correlation function as follows:

$$\alpha^-(\omega) = -\frac{E_0^2}{3}\frac{\omega}{v}\sum_{\eta=x,y,r}(m_\eta^+)^2 G''_\omega(a_\eta^+, a_\eta^+),$$

$$\alpha^{+-}(\omega) = -\frac{E_0^2}{3}\frac{\omega}{v}\sum_{\eta=x,y}(m_\eta^{-+})^2 G''_\omega(a_\eta a_r^+, a_\eta a_r^+),$$

$$\alpha^{--}(\omega) = -\frac{E_0^2}{3}\frac{\omega}{v}\sum_{\eta=x,y}(m_\eta^{++})^2 G''_\omega(a_\eta^+ a_r^+, a_\eta^+ a_r^+). \qquad (20)$$

In order to solve Eqs. (20) we need Eq. (17). The matrix elements in Eq. (17) can be evaluated using the procedure of Ref. 19. We find that

$$G_\omega(a_\eta^+, a_\eta^+) = \sum_{\nu_1}\frac{h_\eta^+(\nu_1)}{\omega_\eta - \omega - B(\nu_1)}, \quad \eta = x, y, r, \qquad (21)$$

$$G_\omega(a_\eta a_r^+, a_\eta a_r^+)$$
$$= \sum_{\nu_1}\frac{h_\eta^{-+}(\nu_1)}{\omega_r - \omega_\eta - \omega - B(\nu_1)}, \quad \eta = x, y, \qquad (22)$$

and

$$G_\omega(a_\eta^+ a_r^+, a_\eta^+ a_r^+)$$
$$= \sum_{\nu_1}\frac{h_\eta^{++}(\nu_1)}{\omega_r + \omega_\eta - \omega - B(\nu_1)}, \quad \eta = x, y. \qquad (23)$$

The $h(\nu_1)$ functions as well as the complex quantity $B(\nu_1)$ = $-\Delta(\nu_1) - i\Gamma(\nu_1)$ are given in the Appendix. The nonvanishing terms in the $\nu_1$ summations might be different for each $\alpha$. The function $B(\nu_1)$ contains all the dynamical information due to the libron–phonon interaction. The real part is connected with the shifts of the absorption lines and the imaginary part with the IR linewidth. The $\nu_1$ = $(n_{1x}, n_{1y}, n_{1r})$ dependence in $B(\nu_1)$ includes all those states that can be reached in a dipolar transition. Since available experiments are spectra in the near IR region[3,5] we study the fundamental vibrational transition $0 \rightarrow 1$. Once we fix $n_{1r} = 1$, $B(\nu_1)$ reduces to $B(n_{1x}, n_{1y}, 1)$ in the near IR region of the spectrum and to $B(n_{1x}, n_{1y}, 0)$ in the far IR. If we further assume that the two librators $x$ and $y$ have the same frequency and the same coupling constant with phonons ($\omega_x = \omega_y$, $\lambda_x = \lambda_y$), then the $n_{1x}, n_{1y}$ dependence of $B$ can be equivalently given in terms of a single index $n$:

$$B(n_{1x}, n_{1y}, v) = B(n, 0, v) = B(0, n, v), \qquad (24)$$

where $n = 0, 1 \cdots$ and $v = 0, 1$.

To obtain numbers out of the expressions for the different components (21)–(23) of the absorption coefficient we need to calculate $B(\nu_1)$ given in Eq. (A8). This equation has two summations, one runs over the $\nu_3$ states and the other over $\mathbf{k}$ states. The first sum can be carried out explicitly in all the $\alpha(\omega)$. For simplicity, $\mathbf{k}$ summations

were performed within the continuous approximation using Debye's model, but other models for the longitudinal phonon density of states could have been used. The following results were obtained.

$$B(n, 0, v) = -\Delta(n, 0, v) - i\Gamma(n, 0, v), \qquad (25)$$

where $v = 0, 1$ and

$$\Delta(n, 0, 0) = -\lambda_x^2 \frac{18}{\nu_D} [-(n-2)f(2\Omega_x - \Omega) + nf(-\Omega)],$$

$$\Delta(n, 0, 1) = -\lambda_x^2 \frac{18}{\nu_D} [(n+2)f(\Omega_x) + nf(-\Omega_x)],$$

$$\Gamma(n, 0, 0) = \lambda_x^2 \frac{18\pi}{\nu_D} [-(n-2)g(2\Omega_x - \Omega) + ng(-\Omega)],$$

$$\Gamma(n, 0, 1) = \lambda_x^2 \frac{18\pi}{\nu_D} [(n+2)g(\Omega_x) + ng(-\Omega_x)]. \qquad (26)$$

Here $\Omega = \omega/\omega_D$, $\Omega_x = \omega_x/\omega_D$, $\omega_D = 2\pi\nu_D$, and

$$f(\Omega) = \int_{-1}^{1} \frac{t(\cos 2\pi t - 1)^2}{\Omega - t} (e^{\gamma t} - 1)^{-1} dt,$$

$$g(\Omega) = \Omega(\cos 2\pi\Omega - 1)^2 (e^{\gamma \Omega} - 1)^{-1}, \qquad (27)$$

with $\gamma = \Theta_D/T$, $\hbar\omega_D = k_B\Theta_D$; $k_B$ is Boltzmann's constant and $\Theta_D$ is Debye's temperature. Going back to Eqs. (20), we now obtain the final result for the absorption coefficient components

$$\alpha^-(\omega) = \Lambda\mu_0^2\left(\frac{x_0}{r_e}\right)^2 (1 - e^{-\beta\hbar\omega_x}) \sum_{n=0}^{n\,\text{max}} \frac{\omega\Gamma(n+1, 0, 0)(n+1)(n+2)e^{-\beta\hbar\omega_x n}}{[\omega_x + \Delta(n+1, 0, 0) - \omega]^2 + \Gamma^2(n+1, 0, 0)} \qquad \text{far IR}$$

$$+ \Lambda\mu_1^2 r_0^2 \sum_{n=0}^{n\,\text{max}} \frac{\omega\Gamma(n, 0, 1)(1+n)e^{-\beta\hbar\omega_x n}}{[\omega_r + \Delta(n, 0, 1) - \omega]^2 + \Gamma^2(n, 0, 1)}$$

$$\alpha^{+-}(\omega) = \Lambda\mu_1^2 r_0^2 \left(\frac{x_0}{r_e}\right)^2 e^{-\beta\hbar\omega_x} \sum_{n=0}^{n\,\text{max}} \frac{\omega\Gamma(n, 0, 1)(n+1)(n+2)e^{-\beta\hbar\omega_x n}}{[\omega_r - \omega_x + \Delta(n, 0, 1) - \omega]^2 + \Gamma^2(n, 0, 1)} \qquad \text{near IR,}$$

$$\alpha^{--}(\omega) = \Lambda\mu_1^2 r_0^2 \left(\frac{x_0}{r_e}\right)^2 \sum_{n=0}^{n\,\text{max}} \frac{\omega\Gamma(n+1, 0, 1)(n+1)(n+2)e^{-\beta\hbar\omega_x n}}{[\omega_r + \omega_x + \Delta(n+1, 0, 1) - \omega]^2 + \Gamma^2(n+1, 0, 1)} \qquad (28)$$

where we have defined $\Lambda \equiv E_0^2/3v$, assumed $\omega_x = \omega_y \ll \omega_r$, and $\beta = 1/k_BT$.

The near IR spectrum profile is given by the last term of $\alpha^-(\omega)$, $\alpha^{+-}(\omega)$, and $\alpha^{--}(\omega)$. Each of these functions, as shown in Eqs. (28), is a superposition of $n_{\text{max}}$ terms as indicated schematically in Fig. 2. In this spectral region, each term in the $n$ summation is a Lorentzian-like function, because $\Delta$ and $\Gamma$ are slowly varying with $\omega$. The Lorentzian maxima and widths depend on both the librational frequency $\omega_x$ and the libron–phonon coupling $\lambda_x$. The envelope of $n_{\text{max}}$ Lorentzians in each of the three absorption coefficient components of Eqs. (28) give the final shape of this spectrum. In the far IR [first term of $\alpha^-(\omega)$] the functions $\Delta$ and $\Gamma$ are not slowly varying with

$\omega$ and consequently the terms in the $n$ summation are not Lorentzians.

In the far, as well as near IR, the functions $\Delta$ and $\Gamma$ are temperature dependent according to Eqs. (26). Notice also that each term in the summations of Eqs. (28) is modulated by a Boltzmann factor. In the range 80–120 K, and for elements with $\Theta_D$ in that temperature region, $\Gamma$ and $\Delta$ dependence with $T$ is small. This means that most of the temperature dependence is due to the exponential weights, i.e., for each Lorentzian in the first term of $\alpha^-(\omega)$ the width decays exponentially with $1/T$:

$$\Gamma_n \sim \Gamma(n, 0, 1)(1 + n)\exp(-\hbar\omega_x n/kT). \qquad (29)$$
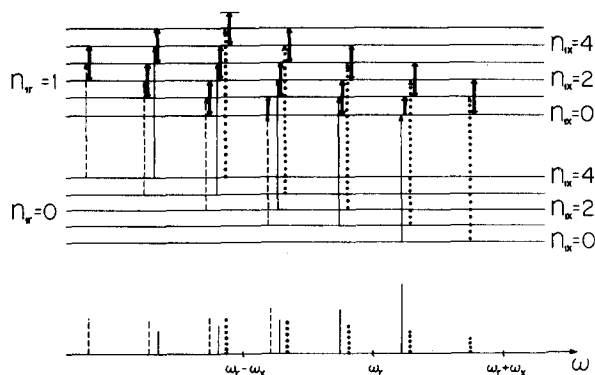
FIG. 2. Schema of the transitions contributing to the absorption coefficient, Eq. (28). Full lines represent terms summed in $\alpha^-(\omega)$, dashed lines correspond to terms summed in $\alpha^{+-}(\omega)$, and dotted lines to terms summed in $\alpha^{--}(\omega)$. The heavy doubled arrowed lines indicate librational levels connected through the libron–phonon coupling that contribute to the functions $\Delta$ and $\Gamma$.

Examination of the envelope width is more involved, since for different systems the $n_{max}$ Lorentzians will be centered at different frequencies.

The parameters in Eqs. (28) are three, the librational frequency $\omega_x$, the libron–phonon coupling constant $\lambda_x$, and the $n$ maximum value $n_{max}$. The latter indicates the number of librational transitions before $D$ starts to rotate freely, i.e., $n_{max}$ is a measure of the cage potential barrier $V_0$ since $n_{max} - 1/2 < V_0/\hbar\omega_x < n_{max} + 1/2$. Whenever $\omega_x$ has a small value, the $n_{max}$ terms in Eq. (28) will be sharp and closely spaced giving a structured envelope. Larger values of $\omega_x$ tend to smooth over the band profile. For fixed $\omega_x$, the widths and shifts towards the red of the terms in the central and high frequency components increase with increasing $\lambda_x$. On the basis of this calculation these parameters can be fitted to experiments where the high orientation sensitivity of the solute has a prevailing importance in determining the absorption band profile.

## IV. COMPARISON WITH EXPERIMENT AND DISCUSSION

The criterion that we follow for the parameter fit is to reproduce the position of the central peak as well as its width for only one temperature. The latter is chosen to be near the solvent $\Theta_D$. Here the parameters were changed one at a time until obtaining a reasonable agreement. A more refined statistical analysis of the data is possible and would be very convenient if one would have the original experimental data.

Chandler and Ewing[3] measured the absorption coefficient for CO in liquid argon. Naulin et al.[5] performed similar experiments for ClF in Ar solution. Both experiments were carried out near 85 K. The CO–Ar system exhibits a maximum band with a weak broad shoulder towards the high frequency region, whereas only one band is clear in the ClF–Ar case. We choose these two examples because they correspond to two molecules with different moment of inertia in liquid argon at a temperature very close to the latter $\Theta_D = 85$ K.[20] The theoretical

model should be better for the CO–Ar system, since CO is lighter than the solvent and has a large moment of inertia. Figure 3 depicts the experimental bands (upper curves) and the theoretical curves generated with the parameters of Table I (lower curves).

If the spectrum of CO in Ar is recalculated at higher temperatures but using the set of parameters already obtained, then the band will be broader and less shifted towards the red. At 97 K the calculation compares very well to the results of Buontempo et al., giving a band very similar to that shown in Fig. 3(a) but shifted and wider by 1 cm$^{-1}$. These authors also reported results for CO in liquid $N_2$ at 84 K. We might attempt a comparison to this other solvent, although we know that now the previous parameter fit will not be adequate, since $N_2$ is a different solvent than argon. Furthermore, $N_2$ is a molecular liquid, has quadrupole and induced absorption and its $\Theta_D = 79$ K. Such trial yields a wider band than in the argon case, which is the correct behavior.

The fit to the experiment of Naulin et al. was done only for $^{35}$ClF, the lighter isotope. Using the parameters from this fit, we calculate the band corresponding to the heavier isotope $^{37}$ClF, obtaining agreement as can be seen in Fig. 3(b), although the whole profile for this case is too structured. Changing the temperature in the 70–120 K range, and keeping the parameters as reported in Table I, we can also reproduce the envelope maximum and width temperature dependence: the band is shifted by about 1 cm$^{-1}$ and the broadening decreases with decreasing temperature. In addition to ClF in argon, Naulin et al. achieved experiments of this solute in liquid $N_2$ and $O_2$. They pointed out from their results that in these solvents there might be interactions yielding associated species such as ClF–$N_2$. Such effects are not included in our solvent cage approach, thus further comparison is not realistic.

When the molecule reaches an energy greater than $V_0$, it has an almost free rotation within the liquid
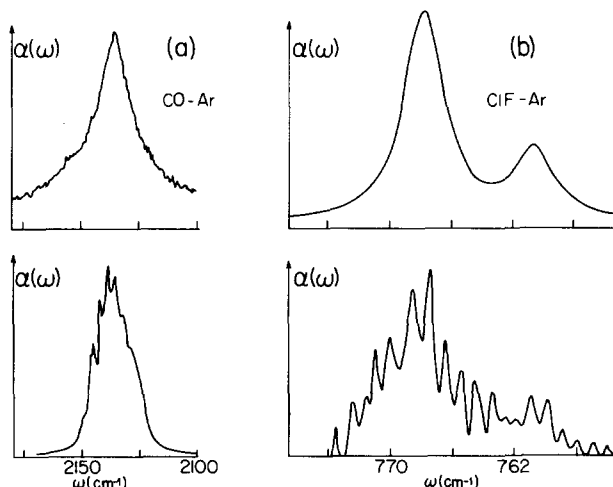


FIG. 3. Near IR absorption bands of (a) CO in Ar at $T = 85$ K; the upper curve is the Chandler and Ewing (Ref. 3) experiment, the lower curve is our result. (b) ClF in Ar at $T = 83$ K; upper curve corresponds to the measurement of Naulin et al. and lower one is our result.

TABLE I. Constants and parameters obtained from the fit of Eqs. (28) to the IR absorption of CO and ClF in liquid argon. For Ar $\Theta_D = 85$ K[20].

|  | $\omega_x$ (cm$^{-1}$) | $n_{max}$ | $V_0$ (cm$^{-1}$) | $\lambda_x$ (cm$^{-1}$) | $\omega_r$ (cm$^{-1}$) | $r_e$ (Å) | $m_{AB}$ |
|---|---|---|---|---|---|---|---|
| CO | 7.5 | 4 | 34 | 1.8 | 2143.5[a] | 1.128[a] | 7.2[a] |
| $^{35}$ClF | 2.5 | 6 | 16 | 0.5 | 773.5[b] | 1.628[b] | 12.2[b] |

[a] Reference 21.
[b] Reference 22.

solution. Such rotational spectrum is not included in the calculated bands of Fig. 3, but should be responsible for part of the wings in the experimental lines.

According to the parameter values obtained by fitting the experiments, we can say that the libron–phonon strength is small (about 0.5–1.8 cm$^{-1}$) but enough to produce a measurable shift and broadening of the spectral lines. As in the calculation we considered only the harmonic approximation for the interaction Hamiltonian, effects such as anharmonicities in the static cage potential or higher order terms in the libron–phonon interaction were neglected. These terms may have an influence in systems where $V_0$ is larger than what we obtained here.

The far IR spectrum for CO in liquid argon at 90 K predicted by our theory with the values $\omega_x$, $\lambda_x$, and $n_{max}$ of Table I is sketched in Fig. 4. The intense broad band at $\nu \sim 50$ cm$^{-1}$ is a superposition of $\Omega$ dependent functions, not Lorentzians, due to the strong $\Omega$ dependence of $\Gamma(n, 0, 0)$ and $\Delta(n, 0, 0)$ in this spectral region. Here again, our results are in agreement with the measurements of Buontempo et al.,[2] although to truly compare with experiments in the far IR, we should include the perturbed rotational spectrum above $V_0$, as well as the effect of quadrupole transitions.

The spectrum of pure liquid CO at 80 K is very similar to that reported for solutions of CO in noble-gas liquids or in N$_2$.[23] As already discussed in this section, the shift and width of the band centered at the diatomics $v = 0 \rightarrow v = 1$ vibrational transition is a consequence of the libron–phonon interaction. Subject to certain modifications, the same framework can be extended to include cage effects when the solvent is a molecular liquid. The largest modification might come from the libron–phonon coupling since collective variables other than translations can occur in molecular liquids.
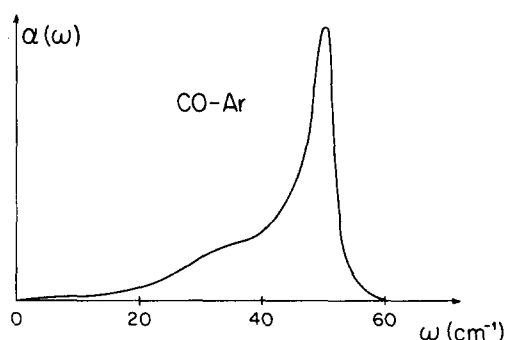
In summary, the IR spectra of diatomics in simple liquids can be interpreted in terms of the coupling between the diatomic libration and the liquid collective motions. The coupling constant values extracted from experiments are small, confirming the hypothesis that the libron–phonon coupling is indeed a small perturbation. Moreover, the values obtained for the librational barrier $V_0$ are of the order of magnitude of those reported in the literature.[4,24]

The present approach has the merit that although it contains three parameters they have a precise meaning: $\omega_x$ and $V_0$ are the librational frequency and height of the static potential, and $\lambda_x$ is the libron–phonon coupling. It represents an improvement over phenomenological treatments, classical calculations with quantum corrections, or theories that consider only the static contribution of the cage. This study suggests the need of more absorption experiments in the far infrared region. Once the parameters are obtained from the near infrared spectrum, the dipolar contribution to the absorption in the far infrared region can be predicted. If more detailed experimental data were available, this calculation could be improved by taking into account additional terms in the libron–phonon interaction, two phonon processes and more realistic phonon frequency distributions.

## ACKNOWLEDGMENTS

## APPENDIX

The constants in Eq. (10) for $\eta = x, y$ are given by

$$m_\eta^+ = m_\eta^- = \mu_0 \frac{\eta_0}{r_e},$$

$$m_\eta^{++} = m_\eta^{+-} = m_\eta^{-+} = m_\eta^{--} = \mu_1 r_0 \frac{\eta_0}{r_e}, \qquad (A1)$$

where $\eta_0 = (\hbar/2m_{AB}\omega_\eta)^{1/2}$ and $r_0 = (\hbar/2m_{AB}\omega_r)^{1/2}$. When $\eta = z$

$$m_z^+ = m_z^- = \mu_1 r_0,$$

$$m_z^{++} = m_z^{+-} = m_z^{-+} = m_z^{--} = 0. \qquad (A2)$$

The current density operator expression analogous to Eq. (10) is

$$J_\eta = j_\eta^+ a_\eta^+ + j_\eta^- \alpha_\eta + j_\eta^{++} a_\eta^+ a_r^+$$

$$+ j_\eta^{+-} a_\eta^+ a_r + j_\eta^{-+} a_\eta a_r^+ + j_\eta^{--} a_\eta a_r, \qquad (A3)$$



FIG. 4. Dipolar contribution to the far IR spectrum of CO in Ar as obtained from this calculation using the parameter values given in Table I.

where for $\eta = x, y$,

$$j_\eta^+ = -j_\eta^- = i\mu_0 \frac{\eta_0}{r_e} \omega_\eta,$$

$$j_\eta^{-+} = -j_\eta^{+-} = i\frac{\mu_1}{r_e} \frac{\hbar}{2m_{AB}} \left[ \left(\frac{\omega_r}{\omega_\eta}\right)^{1/2} - \left(\frac{\omega_\eta}{\omega_r}\right)^{1/2} \right],$$

$$j_\eta^{++} = -j_\eta^{--} = i\frac{\mu_1}{r_e} \frac{\hbar}{2m_{AB}} \left[ \left(\frac{\omega_r}{\omega_\eta}\right)^{1/2} + \left(\frac{\omega_\eta}{\omega_r}\right)^{1/2} \right], \quad (A4)$$

and for $\eta = z$

$$j_z^+ = -j_z^- = i\mu_1 r_0 \omega_r,$$

$$j_z^{++} = -j_z^{--} = j_z^{+-} = -j_z^{-+} = 0. \quad (A5)$$

The functions $h(\nu_1)$ in Eqs. (21)–(24) are given by

$$h_\eta^+(\nu_1) = \frac{\eta_{1\eta}}{\omega_\eta} e^{-\beta \epsilon_{\nu_1}} (1 - e^{\beta \hbar \omega_\eta}) \frac{j_\eta^-}{m_\eta^+}, \quad (A6)$$

where $\eta$ can take the three values $x$, $y$, or $r$. Also

$$h_\eta^{-+}(\nu_1) = \frac{n_{1r}(n_{1\eta} + 1)}{\omega_r - \omega_\eta} e^{-\beta \epsilon_{\nu_1}} [1 - e^{\beta \hbar(\omega_r - \omega_\eta)}] \frac{j_\eta^{+-}}{m_\eta^{-+}},$$

$$h_\eta^{++}(\nu_1) = \frac{n_{1r} n_{1\eta}}{\omega_r + \omega_\eta} e^{-\beta \epsilon_{\nu_1}} [1 - e^{\beta \hbar(\omega_r + \omega_\eta)}] \frac{j_\eta^{--}}{m_\eta^{++}} \quad (A7)$$

but with $\eta = x$ or $y$ only. Equation (18) gives the expression for $\epsilon_{\nu_1}$. The expression for $B(\nu_1)$ is given by

$$B(\nu_1) = \sum_{\eta=x,y} \lambda_\eta^2 \sum_k \sum_{\nu_3} (1 + n_k) \Big\{ (\gamma_k)_{13} [(\gamma_k^+)_{31} - A_{31,12}(\gamma_k^+)_{12}]$$

$$\times \frac{1}{\epsilon_{32} + \omega_k - \omega + ia} + (\gamma_k^+)_{12} [(\gamma_k)_{21}$$

$$- A_{31,12}(\gamma_k)_{13}] \frac{1}{\epsilon_{11} - \omega_k - \omega + ia} \Big\}$$

$$+ \sum_{\eta=x,y} \lambda_\eta^2 \sum_k \sum_{\nu_3} n_k \Big\{ (\gamma_k^+)_{13} [(\gamma_k)_{31} - A_{31,12}(\gamma_k)_{12}]$$

$$\times \frac{1}{\epsilon_{32} - \omega_k - \omega + ia}$$

$$+ (\gamma_k)_{12} [(\gamma_k^+)_{21} - A_{31,12}(\gamma_k^+)_{13}] \frac{1}{\epsilon_{11} + \omega_k - \omega + ia} \Big\}$$

$$(A8)$$

Here $A_{31,12} = (A_\eta)_{31}/(A_\eta)_{12}$, $\gamma_k = (\omega_D/\omega_k)^{1/2} F_\eta(k)(a_\eta^+ + a_\eta)$, and where $A_\eta$ is either $a_\eta^+$, $a_\eta^+ a_r^+$, or $a_\eta a_r^+$ and $n_k = (e^{\beta \hbar \omega_k} - 1)^{-1}$.

[1] R. Coulon, L. Galatry, B. Okseengorn, S. Rubin, and B. Vodar, J. Phys. Radium 15, 641 (1954).

[2] U. Buontempo, S. Cunsolo, and G. Jacucci, J. Chem. Phys. 59, 3750 (1973).

[3] D. W. Chandler and G. E. Ewing, Chem. Phys. 54, 241 (1981).

[4] H. Dubost, Chem. Phys. 12, 139 (1976).

[5] C. Naulin, J. Lambard, and R. Bougon, J. Chem. Phys. 76, 3371 (1982).

[6] P. H. Berens and K. R. Wilson, J. Chem. Phys. 74, 4872 (1981).

[7] J. Manz, J. Am. Chem. Soc. 102, 1801 (1980).

[8] D. Robert and L. Galatry, J. Chem. Phys. 55, 2347 (1971).

[9] F. Mauricio, S. Velasco, C. Girardet, and L. Galatry, J. Chem. Phys. 76, 1624 (1982).

[10] S. Bratos, J. Rios, and Y. Guissani, J. Chem. Phys. 52, 439 (1970).

[11] R. G. Gordon, J. Chem. Phys. 43, 1307 (1965); 44, 1830 (1966).

[12] E. Blaisten-Barojas and M. Allavena, J. Phys. C 9, 3121 (1976).

[13] R. Kubo, J. Phys. Soc. Jpn. 12, 570 (1957).

[14] I. L. Garzón and E. Blaisten-Barojas, Internal Communication, IFUNAM 84-002, pp. 11–21.

[15] S. Fujita, Introduction to Non-Equilibrium Quantum Statistical Mechanics (W. B. Saunders, Philadelphia, 1966) Chaps. 5 and 7.

[16] R. Zwanzig, in Statistical Mechanics: New Concepts, New Problems, New Applications, edited by S. A. Rice, K. F. Freed, and J. C. Light (University of Chicago, Chicago, 1972), p. 229.

[17] E. Blaisten-Barojas and M. Allavena, Int. J. Quantum Chem. 7, 195 (1973).

[18] L. D. Landau and E. M. Lifshitz, Statistical Physics (Pergamon, Oxford, 1959), p. 391.

[19] A. Lodder and S. Fujita, J. Phys. Soc. Jpn. 25, 774 (1968).

[20] N. N. Ashcroft and N. D. Mermin, Solid State Physics (Holt, Rinehart and Winston, New York, 1976).

[21] G. Herzberg, Spectra of Diatomic Molecules (Van Nostrand, New York, 1959).

[22] R. E. Willis, Jr. and W. W. Clark III, J. Chem. Phys. 72, 4946 (1980).

[23] G. E. Ewing, J. Chem. Phys. 37, 2250 (1962).

[24] G. P. Chausov, V. G. Manzhelli, and Yu. A. Freiman, Sov. Phys. Solid State 13, 1248 (1971).